THE JOURNAL OF PHYSICAL CHEMISTRY B

 VOLUME 106, NUMBER 12, MARCH 28, 2002

LETTERS

A New Insight into Nafion Structure

Anne-Laure Rollet, Olivier Diat,* and Gérard Gebel

Département de Recherche Fondamentale sur la Matière Condensée, SI3M, Groupe Polymères Conducteurs Ioniques, CEA-Grenoble 17, rue de Martyrs, 38054 Grenoble Cedex 9, France

Received: January 28, 2002

The structure of hydrated Nafion membranes neutralized by $N(CH_3)_4^+$ ions has been investigated by the small angle neutron scattering technique. First, the spectra show that the counterions are condensed at the interface between hydrophilic and hydrophobic phases. More importantly, by applying a contrast variation method, the normalized scattered intensity of membranes swollen in several D_2O/H_2O mixtures was analyzed. The $N(CH_3)_4^+$ counterions were used as a probe to identify the nature of the scattering entity that is polymeric aggregates surrounded by ionic groups and water molecules, contrary to the generally accepted model. This new insight into the Nafion structure will allow one to reconsider the swelling process and the degree of mesoscopic orientation in such perfluorinated systems.

Introduction

The Nafion (E. I. du Pont de Nemours), whose chemical formula is indicated below is the most studied ionomer

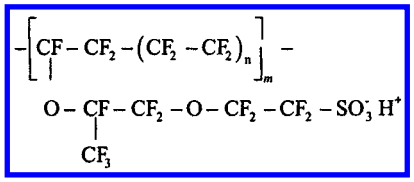

membrane thanks to its good performance in electrochemical devices.[1,2] Its structure, characterized by a microphase separation, has been widely studied using small angle scattering with neutrons (SANS) and X-rays (SAXS).[3−8] The range of transfer momentum q from 0.01 to 0.4 Å^{-1} has been particularly investigated because of the occurrence of the so-called "ionomer peak" at around 0.11 Å^{-1} which is the most striking feature of these spectra. Two other main features are observable: at lower q values ($q \approx 0.02$ Å^{-1}), a shoulder which is up to now not really simulated but associated to the degree of cristallinity of the polymer and, at higher q values ($q > 0.2$ Å^{-1}), the q^{-4} decrease of the scattered intensity, characteristic of the so-called Porod law. Moreover, at very low q values ($q < 10^{-2}$ Å^{-1}), a small angle upturn has been also observed and analyzed considering large scale density inhomogeneities.[9] Despite these numerous studies, Nafion structure is still subject to controversy and several models have been proposed. The most common is the Gierke's one:[10] the polymer is assumed to form reverse micelles (about 20 Å radius) connected by small cylindrical pores (10 Å length, 5 Å radius). The Dreyfus model,[11] designed to analyze SANS and SAXS data, is derived from the Gierke model, with the micelles being organized on a diamond lattice but with a short range order. Cooper et al.[12,13] and Fujimura et al.[14] considered different distributions of the spherical aggregates of sulfonated groups. Other models, that do not consider connected spherical cavities, have also been suggested to describe the structure of the hydrophilic phase of Nafion. For example, Litt,[15,16] analyzing the shift of the ionomer peak with the water volume fraction, described the Nafion structure as a lamellar organization of planar clusters. As well, Verbrugge et

* To whom correspondence should be addressed. E-mail: odiat@cea.fr. Fax: 33 4 38 78 56 91.

10.1021/jp020245t CCC: $22.00
Published on Web 03/03/2002

al.[17] did not agree with the existence of cavities connected by small charged pores because of the high value of the self-diffusion coefficient, measured for HSO_4^- co-ions (about 1.4 10^{-6} cm^2/s). They proposed to describe the hydrophilic phase as a tortuous network assuming monodisperse pores of about 60 Å diameter. On the basis of NMR, ENDOR, and SAXS data, Timashev[18] argued for a similar structure but with thinner pores. More recently, Haubold et al.[19] analyzed their SAXS data considering small oblong unit cells composed by a sandwich of polymer−ionic groups−solvent−ionic groups−polymer. These unit cells are supposed to be linked together, but their model does not take into account their correlation.

All of the previous models whose list here is not exhaustive attempt to describe the structure of the hydrophilic domains of the Nafion membrane but there are still some debates about the processes implied during the ionic clusters reorganization. Our point of view is slightly different. We propose a new comprehensive structural approach for Nafion membrane taking in account the polymer aggregates as the basic scattering entity. This consideration is based on SANS experiments with a contrast variation method using the counterion as a third scatterer. It allows us to discriminate between an "inverse micelle" and a "direct micelle" type structure in order to reconsider the swelling process.

Experimental Section

The Nafion membranes were purchased from Dupont de Nemours. They were first cleaned by immersing successively in concentrated HCl solution and concentrated NaOH solution and rinsed in boiling water during 1 h, and then the membranes were equilibrated with $N(CH_3)_4Cl$ in D_2O solution and with $N(CH_3)_4Cl$ in H_2O solution, to exchange the H^+ counterions with $N(CH_3)_4^+$. Finally, the membranes were washed in pure water several times to remove the excess of salt. It has been shown that the nature and the charge of the counterion has a slight effect on the swelling of the Nafion membrane,[20] but its structure itself does not change, and if the counterion is not to big (it is still the case for $N(CH_3)_4^+$), all the protons are exchanged.

We have used SANS technique to obtain information on the shape of scattering objects of nanometer sizes, and we have varied the scattering contrast between the polymer backbone, the counterions, and the solvent, using several mixtures of H_2O and D_2O. The scattering length density of the solvent ranged from $-0.56\ 10^{10}$ (pure H_2O) to $6.34\ 10^{10}$ cm^{-2} (pure D_2O). In the following, we will denote x as the volume fraction of D_2O in H_2O ($x = V_{D2O}/(V_{D2O} + V_{H2O})$). Experiments were performed on the PAXE spectrometer at the Laboratoire Léon Brillouin (CEA-CNRS, Orphée reactor, Saclay, France). The sample-to-detector distance, D_{SD}, was 1.5 m and the incident wavelength λ was 1.5 m in order to explore $2 \times 10^{-2} < q$ (Å^{-1}) $< 4 \times 10^{-1}$ where q is the neutron momentum transfer ($q = 4\pi \sin\theta/\lambda$ and 2θ is the scattering angle). Four pieces of membrane (total thickness = 880 μm) were stacked in sealed quartz cells (1 mm path length) filled with water in order to avoid drying during measurements. Usual corrections for background subtraction, detector response, and absolute intensity normalization were applied.

Results

The Porod behavior (the q^{-4} intensity decrease), usually observed at lower wave vectors than the ionomer peak one, indicates that the scattering density variation at the interface can be described within a one step variation profile assuming a sharp physical interface between the polymer and the confined solution. It is important to note that this result does not depend on the shape of the scattering object. It can be reasonably thought that the sulfonated groups are located at this sharp interface. The numerous theoretical[21−24] and experimental[25−27] studies of electrostatic interactions in micellar systems have shown that the counterions will condense close to charged surfaces, whatever their geometry (confined or not). A large proportion of the $N(CH_3)_4^+$ counterions are therefore expected to be close to the sulfonated groups. They have been chosen because, due to their 12 protons, they are good neutron scatterers. In the Nafion membranes, they will appear as a third neutron scattering domain with a different scattering contrast with the solvent and the polymer backbone. Then analyzing the SANS spectra corresponding to a different H_2O/D_2O ratio, we determined the contrast profile of the scattering domains and therefor a new insight into the Nafion structure.

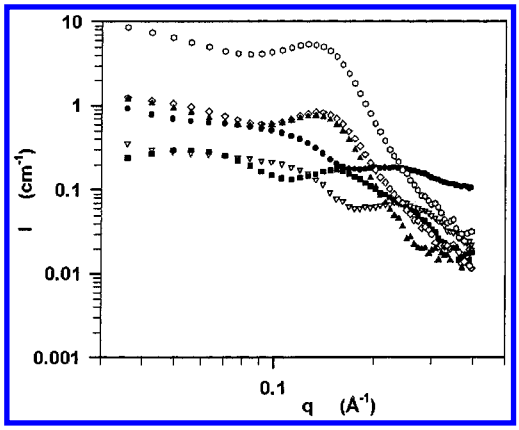

Figure 1. Experimental spectra of Nafion membranes neutralized by $N(CH_3)_4^+$ in several mixtures of D_2O/H_2O ($x = V_{D2O}/(V_{D2O} + V_{H2O})$): $x = 1$ (●), $x = 0.9$ (▽), $x = 0.75$ (■), $x = 0.5$ (◇), $x = 0.25$ (▲), and $x = 0$ (◇).

The spectra of Nafion membranes, neutralized by $N(CH_3)_4^+$ in water, with x varying from 0 to 1, are presented in Figure 1. The shapes of these scattering curves are significantly different: the ionomer peak (q around 0.13 Å^{-1}) observed for membranes in pure H_2O disappears as well as the Porod region when the proportion of D_2O is increased. In the same time, two shoulders appear, one at lower q values (q' around 0.08 Å^{-1}) and one at larger q values (q'' around 0.2 Å^{-1}), and the scattered intensity decreases because of the reduction of contrast between the polymeric domains and the solvent.

Thus, varying the solvent scattering density modifies the scattering profile. This behavior is not observed when the same experiments are performed with acidified membranes, because the contrast with the proton is low. On the other hand, the variation of intensity as a function of q, in Figure 1, shows clearly the effect of the condensation of the $N(CH_3)_4^+$ counterions. They are located in a thin layer with the sulfonated groups at the interface between the hydrophobic polymer parts and the solvent. Such condensation has been already observed in micellar systems,[26,28,29] but it is the first time that it is clearly shown in perfluorosulfonated ionomer films. To analyze the SANS data, the scattering length density profile has been represented by a two steps profile: one step between the polymer and the counterions and a second step between the counterions and the solvent (see Figure 3).

In SANS and SAXS experiments, the scattered intensity can be considered as originating from the combination of a term describing the shape of the aggregates (the form factor, $P(q)$) and a term describing their spatial distribution (the structure

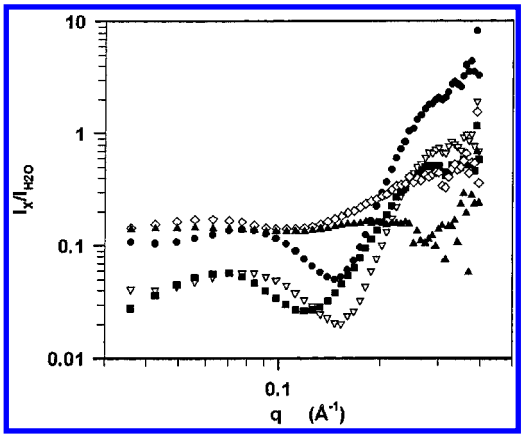

Figure 2. Spectra of Nafion membranes neutralized by $N(CH_3)_4^+$ in several mixtures of D_2O/H_2O ($x = V_{D2O}/(V_{D2O} + V_{H2O})$) normalized by the spectrum of Nafion membrane in pure H_2O ($x = 0$): $x = 1$ (●), $x = 0.9$ (▽), $x = 0.75$ (■), $x = 0.5$ (◇), and $x = 0.25$ (▲).

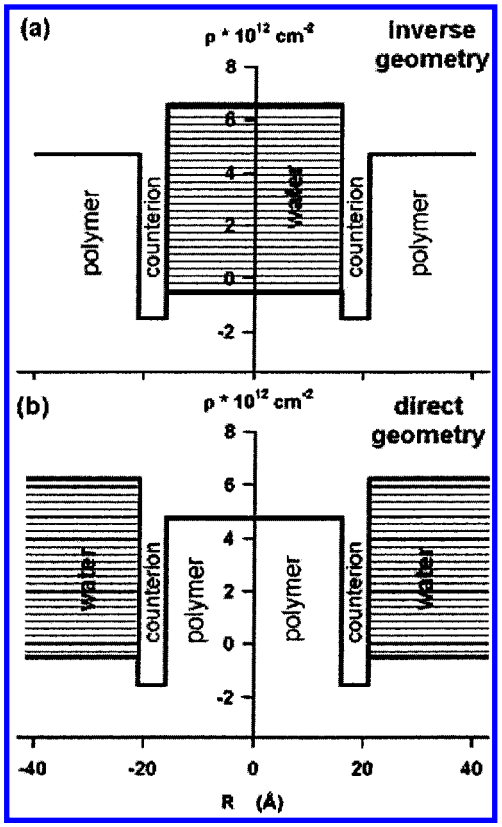

Figure 3. Two-step profiles of the scattering length densities variation at the hydrophilic/hydrophobic interface for two opposite considerations (a) inverse geometry when we consider ionic clusters in a polymer matrix and (b) direct geometry when the electrolyte solution surrounds the polymer aggregate. The hatched parts correspond to the domains where the contrast is varied (from 6.34 10^{10} to -0.5 10^{10} cm^{-2}).

factor, $S(q)$). In the case of spherical aggregates, this combination is simply a product:

$$I(q) = KP(q)\,S(q) \tag{1}$$

where K is a scaling factor taking into account the contrast term and the density of scattering objects. As no structural change occurs when H_2O is replaced by D_2O, the structure factor $S(q)$ in eq 1 is independent of x, whereas the form factor $P(q)$ appears to be modified. To eliminate the structural component $S(q)$, the analysis has been performed on the spectra of Nafion in D_2O/H_2O mixtures (x ranging from 1 to 0.25) normalized by the spectrum of Nafion in pure H_2O ($x = 0$):

$$Y_x = \frac{I_x}{I_0} = \frac{P_x}{P_0} \tag{2}$$

Thanks to this procedure, the analysis is simplified, because no assumption on the spatial distribution is needed. The results are presented in Figure 2. The curves obtained present a clear minimum around 0.15 Å^{-1} that is shifted toward smaller q values when x is decreased.

For several x values, the normalized curves Y_x have been calculated assuming the most simple shape that has been used in several models of Nafion structure,[10−14] i.e., the sphere. The distribution of the ionic species is represented by a corona at the interface between the hydrophobic and the hydrophilic phases. The form factor for spherical core−shell particles is written as follows:

$$P(q) = \{(\rho_{ext} - \rho_{ion})R^3\Phi(qR) + (\rho_{ext} - \rho_{ion})(R \pm t)^3\Phi[q(R \pm t)]\}^2 \tag{3}$$

with

$$\Phi(x) = 3\frac{\sin(x) - x\cos(x)}{x^3} \tag{4}$$

where R is the radius of the sphere (delimited by the hydrophilic/hydrophobic interface); t is the thickness of ion corona; and ρ_{ext}, ρ_{ion}, and ρ_{int} are the scattering length densities of the external medium, of the counterion shell, and of the internal core, respectively.

For the inverse geometry, i.e., when we consider spherical cavities filled with electrolyte solutions in a polymer matrix (models of ref 10−14), we use $(R - t)$ in eq 3 and $\rho_{ext} = \rho_{polymer} = 4.7\ 10^{10}$ cm^{-2} and $\rho_{int} = \rho_{water} = 6.34\ 10^{10}$ cm^{-2} for pure D_2O to $-0.5\ 10^{10}$ cm^{-2} for pure H_2O (see Figure 3a). The scattering length density of the ion is $\rho_{ion} = -1.5\ 10^{10}$ cm^{-2}. Figure 4a shows the calculated Y_x for inverse geometry ($R =$ 15 Å and $t = 4$ Å). The general shape of the calculated curves is similar to the experimental data. However, the deeper minimum of the curves is shifted to higher q values when x is decreased, unlike what is observed experimentally.

The same modeling has been performed for direct geometry (see Figure 3b). We consider in this case spherical aggregates of polymer surrounded by electrolyte solutions. In eq 3, $(R - t)$ has to be replaced by $(R + t)$ and $\rho_{int} = \rho_{polymer}$ and $\rho_{ext} = \rho_{water}$. The function Y_x obtained for direct geometry is presented in Figure 4b. As for the inverse geometry, Y_x also reproduces quite well the general shape of the SANS data but this time the minimum shifts to smaller q values, as experimentally observed.

A simple explanation of this effect is that the scattering object appears to be larger as the protonated solvent H_2O is continuously replaced by D_2O. The effect of the shape of scattering particles has been investigated and similar calculations have been performed for rodlike and ribbonlike particles.[30] Then similar results are obtained, the shape of the curves is close to the experimental data, and the position of the larger minimum shifts to smaller q with respect to x. For a given experimental curve, we can always find a set of fitting parameters for the data, but it must be emphasized that this set is unique as soon as we consider the complete series with different x values.

To verify that no other contrast effect can compensate the shift of the minimum to higher q values in the case of inverse geometry, several tests have been performed. First, if one takes

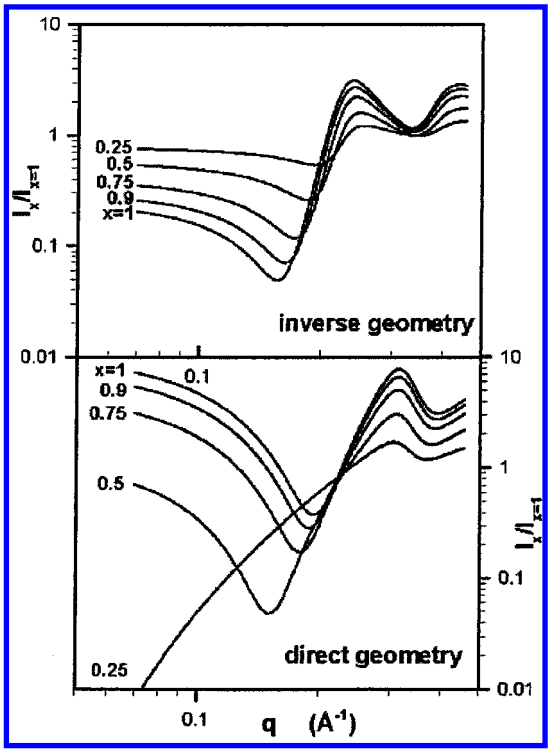

Figure 4. Theoretical curve of I_X/I_{H2O} ($x = V_{D2O}/(V_{D2O} + V_{H2O})$) for spherical shapes with direct and inverse geometry with a corona of $N(CH_3)_4^+$ in each case. The x values are indicated on the graphs.

into account a change of scattering length density of the counterion corona because of the hydration of the counterion when the contrast of the solvent is varied, then the shift of the minimum to higher q values is even more pronounced. One could also assume a second scattering density corona corresponding to the hydration of the sulfonated groups between the polymer and the counterion corona. For inverse geometry, the shift to higher q is then less pronounced, but the shape of the theoretical curves does not look like the experimental one anymore. In the model of Hsu et al. and Dreyfus et al., small water pores (5 Å length and diameter) are assumed to be connected with cylindrical hydrophilic cavities. In a SANS experiment, such cavities cannot be observed directly, nevertheless they could contribute to the scattering. We have taken into account their influence in two different ways: first, we have to considered that the apparent scattering length density of the polymer is modified when the contrast of the solvent is changed, and second, we have considered two kind of spheres: the pores (radius 20 Å) and the cavities (radius 5 Å). Whatever the assumptions, this effect cannot lead to a shift of the minimum to a smaller q value for inverse geometries. Thus, considering the hydrated Nafion structure as an assembly of polymeric aggregates surrounded with the counterions and the water molecules, we should analyze the swelling process in a different way, taking into account that the ionomer peak corresponds to the mean distance between these particles. An accurate determination of the shape and the distribution of these aggregates will allow one to characterize more precisely the mechanical, optical (birefringence), and transport properties in such material.

Conclusion

The hydrated Nafion membrane contains highly segregated nanodomains. The fixed sulfonated groups are located at their interfaces, and the $N(CH_3)_4^+$ counterions are condensed on this charged surface, as it is shown by our SANS spectra. To analyze the different SANS spectra obtained using a contrast variation method, we have assumed several scattering geometries: spherical or elongated cavities filled by electrolyte solution and spherical or rod-like aggregates of polymer surrounded by the electrolyte solution. The best description of SANS data is obtained with the aggregates of polymer. However, it is not possible to distinguish between spherical and rodlike aggregates at this point because the scattering range is too limited. The analysis of Nafion structure over a wider range of q values will constitute a following work.

Acknowledgment. The authors are grateful to the Laboratoire Léon Brillouin for providing neutron beam time and to J. Teixeira, their local contact, for his help with the SANS experiments.

References and Notes

(1) Schlick, S. *Ionomers: characterization, theory and applications*; CRC Press: Boca Raton, FL, 1996.

(2) Eisenberg, A.; Yeager, H. L. *Perfluorinated Ionomer Membranes*, ACS Symposium, Series 180; American Chemical Society: Washington, DC, 1982.

(3) Roche, E. J.; Pineri, M.; Duplessix, R.; Levelut, A. M. *J. Polym. Sci. Polym. Phys. Ed.* **1981**, *19*, 1−11.

(4) Gierke, T. D.; Munn, G. E.; Wilson, F. C. *J. Polym. Sci. Polym. Phys. Ed.* **1981**, *19*, 1687−1704.

(5) Elliott, J. A.; Hanna, S.; Elliott, A. M. S.; Cooley, G. E. *Macromolecules* **2000**, *33*, 4161−4171.

(6) Gebel, G.; Moore, R. B. *Macromolecules* **2000**, *33*, 4850−4855.

(7) Loppinet, B.; Gebel, G.; Williams, C. E. *J. Phys. Chem. B* **1997**, *101*, 1884−1892.

(8) Gebel, G. *Polymer* **2000**, *41*, 5829−5838.

(9) Gebel, G.; Lambard, J. *Macromolecules* **1997**, *30*, 7914−7920.

(10) Hsu, W. Y.; Gierke, T. D. *J. Membrane Sci.* **1983**, *13*, 307.

(11) Dreyfus, B.; Gebel, G.; Aldebert, P.; Pineri, M.; Escoubes, M.; Thomas, M. *J. Phys. France* **1990**, *51*, 1341−1354.

(12) Yarusso, D. J.; Cooper, S. L. *Macromolecules* **1983**, *16*, 1871.

(13) Yarusso, D. J.; Cooper, S. L. *Polymer* **1985**, *26*, 371.

(14) Fujimura, M.; Hashimoto, T.; Kawai, H. *Macromolecules* **1982**, *15*, 136−144.

(15) Litt, M. H. *Polym. Prep.* **1997**, *38*, 80−81.

(16) Litt, M. H. *Book of Abstract*, 213th ACS National Meeting Symposium; American Chemical Society: Washington, DC, 1997.

(17) Verbrugge, M. W.; Hill, R. F. *J. Electrochem. Soc.* **1990**, *137*(3), 893−899.

(18) Timashev, S. F. *Physical Chemistry of Membrane Process*; Ellis Horwood Series in Physical Chemistry; Ellis Horwood: New York, 1991.

(19) Haubold, H.-G.; Vad, T.; Jungbluth, H.; Hiller, P. *Electrochim. Acta* **2001**, *46*, 1559−1563.

(20) Rollet, A. L.; Gebel, G.; Simonin, J. P.; Turq, P. J. *Polym. Sci.: Part B* **2001**, *39*, 548−558.

(21) Akoum, F.; Parodi, O. *J. Phys.* **1985**, *46*, 1675.

(22) Bratko, D.; Luzar, A.; Chen, S. H. *J. Chem. Phys.* **1988**, *89*, 545.

(23) Brown, D.; Clarke, J. H. R. *J. Phys. Chem.* **1988**, *92*, 2881.

(24) Bratko, D. *Chem. Phys. Lett.* **1990**, *169*(6), 555.

(25) Chen, S. H. *Annu. Rev. Phys. Chem.* **1986**, *37*, 351−399.

(26) Wu, C. F.; Chen, S. H.; Shih, L. B.; Lin, J. S. *J. Appl. Cryst.* **1988**, *21*, 853−857.

(27) Linse, P.; Halle, B. *Mol. Phys.* **1989**, *67*(3), 537−573.

(28) Chen, S.; Liu, Y. C. *Polym. Mater. Sci. Eng.* **1994**, *71*, 702−703.

(29) Chang, S.-L.; Ku, C.-Y.; Chen, S.-H.; Lin, J. S. *J. Phys. IV* **1993**, *3*(C8), 117−127.

(30) For these latter cases, eq 1 is not anymore valid except if we consider that we restrict the evaluation to the scattering domain with $Lq \gg 1$, with L being the length of rods or ribbons.